

See discussions, stats, and author profiles for this publication at: <https://www.researchgate.net/publication/7063701>

Effects of Natural Water Ions and Humic Acid on Catalytic Nitrate Reduction Kinetics Using an Alumina Supported Pd–Cu Catalyst

ARTICLE *in* ENVIRONMENTAL SCIENCE AND TECHNOLOGY · JUNE 2006

Impact Factor: 5.33 · DOI: 10.1021/es0525298 · Source: PubMed

CITATIONS

65

READS

59

5 AUTHORS, INCLUDING:



Brian P Chaplin

University of Illinois at Chicago

28 PUBLICATIONS 431 CITATIONS

SEE PROFILE



John R Shapley

University of Illinois, Urbana-Champaign

253 PUBLICATIONS 6,203 CITATIONS

SEE PROFILE

Effects of Natural Water Ions and Humic Acid on Catalytic Nitrate Reduction Kinetics Using an Alumina Supported Pd–Cu Catalyst

BRIAN P. CHAPLIN,[†] ERIC ROUNDY,^{†,§}
KATHRYN A. GUY,[‡]
JOHN R. SHAPLEY,[‡] AND
CHARLES J. WERTH^{*,†}

Department of Civil and Environmental Engineering, and
Department of Chemistry, University of Illinois at
Urbana-Champaign, Urbana, Illinois 61801

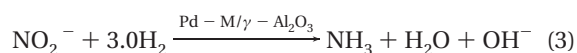
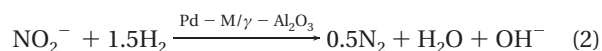
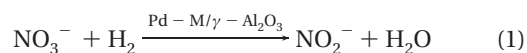
Catalytic nitrate reduction was evaluated for the purpose of drinking water treatment. Common anions present in natural waters and humic acid were evaluated for their effects on NO₃[−] hydrogenation over a bimetallic supported catalyst (Pd–Cu/γ-Al₂O₃). Groundwater samples, with and without powder activated carbon (PAC) pretreatment, were also evaluated. In the absence of inhibitors the NO₃[−] reduction rate was 2.4 × 10^{−01} L/min g cat. However, the addition of constituents (SO₄^{2−}, SO₃^{2−}, HS[−], Cl[−], HCO₃[−], OH[−], and humic acid) on the order of representative concentrations for drinking water decreased the NO₃[−] reduction rate. Sulfite, sulfide, and elevated chloride decreased the NO₃[−] reduction rate by over 2 orders of magnitude. Preferential adsorption of Cl[−] inhibited NO₃[−] reduction to a greater extent than NO₂[−] reduction. Partial regeneration of catalysts exposed to SO₃^{2−} was achieved by using a dilute hypochlorite solution, however Cu dissolution occurred. Dissolved constituents in the groundwater sample decreased the NO₃[−] reduction rate to 3.7 × 10^{−03} L/min g cat and increased ammonia production. Removal of dissolved organic matter from the groundwater using PAC increased the NO₃[−] reduction rate to 5.06 × 10^{−02} L/min g cat and decreased ammonia production. Elemental analyses of catalysts exposed to the natural groundwater suggest that mineral precipitation may also contribute to catalyst fouling.

1. Introduction

Nitrate (NO₃[−]) is the world's most widespread groundwater contaminant (1), mainly resulting from natural and man-made fertilizers. Consumption of NO₃[−] can lead to a fatal condition called methemoglobinemia, or "blue baby syndrome" (2). Nitrite may also form N-nitroso compounds, which are known carcinogens (3). For these reasons, regulatory agencies have established maximum contaminant levels (MCL) of 10 mg/L NO₃[−] N (44 mg/L as NO₃[−]) (4) and 11.3 mg/L NO₃[−] N (50 mg/L as NO₃[−]; European Community) (5).

Several physicochemical and biological processes are available to remove NO₃[−], including ion exchange, electrodialysis, reverse osmosis, and biological denitrification. However, physicochemical processes produce a concentrated brine that must be treated or wasted, and biological denitrification for drinking water is limited because of concerns with pathogens, turbidity, and chlorine demand for the treated water (6).

Catalytic NO₃[−] reduction has received attention as a possible solution to these problems. Catalysts comprised of Pd–Cu, Pd–In, and Pd–Sn have been shown to actively reduce NO₃[−] when added to a solution along with hydrogen as an electron donor (7–23). This catalytic reduction results in the production of nitrogen (N₂) gas and ammonia (NH₃), and NO₂[−] as an intermediate. Intermediates such as NO and N₂O have also been proposed (11, 13), but only N₂O has been detected (11, 13, 18). The proposed catalytic reactions are as follows, where M represents the second metal:



A dual site model consisting of preferred sites for NO₃[−] and NO₂[−] reduction has been proposed in the literature (10, 15, 24), but has not been confirmed. The USEPA has set an MCL for NO₂[−] at 1.0 mg/L as N (4), and in the European Community the maximum permitted levels for NO₂[−] and NH₃ are 0.1 mg/L as NO₂[−] and 0.5 mg/L as NH₄⁺, respectively.

Catalytic NO₃[−] reduction proceeds rapidly (i.e., half-life of tens of minutes) when distilled water is the reaction medium. However, natural water can cause a substantial decrease in catalytic NO₃[−] reduction efficiency (10, 12, 13). Several solutes in natural waters may be responsible for this decrease. Elevated OH[−] concentrations have been shown to increase the concentrations of NO₂[−] and NH₃ after a given reaction time (7, 10, 13, 14, 16, 18, 19, 21). Studies have shown that HCO₃[−] inhibits NO₃[−] reduction (10, 12, 14). Chloride has been shown to inhibit NO₃[−] reduction at high concentrations (≥2500 mg/L) (23). Studies have shown that SO₄^{2−} and CO₃^{2−} do not significantly affect NO₃[−] reduction rates (17, 20).

The effect of reduced sulfur species and humic acid on catalytic NO₃[−] reduction has not been investigated. Bacteria under anaerobic conditions can form reduced sulfur species such as SO₃^{2−}, SO₂[−], HS[−], S^{2−}, and S_(s) that are known catalyst poisons (25–30). Organics (such as humic acid) are known to complex with metals and metal oxides (31), and could inhibit NO₃[−] reduction.

In this study, Pd–Cu on γ-Al₂O₃ catalysts was prepared and tested in a slurry batch reactor. Common anions in natural waters (CO₃^{2−}, HCO₃[−], H₂CO₃, Cl[−], SO₄^{2−}, SO₃^{2−}, HS[−]) and humic acid were added to deionized Nanopure water (DNW), and evaluated for their ability to inhibit catalytic NO₃[−] reduction in the presence of H₂. Groundwater samples, before and after pretreatment with PAC, were also evaluated to determine the effects of pretreatment on NO₃[−] removal. The resulting NO₃[−] reduction rates and final NO₂[−] and NH₃ concentrations were compared to determine which solutes affect catalytic NO₃[−] reduction in real drinking waters. Regeneration of Pd–Cu catalysts were also tested to assess the longevity of these catalysts.

* Corresponding author phone: 217-333-3822; fax: 217-333-6968; e-mail: werth@uiuc.edu.

[†] Department of Civil and Environmental Engineering.

[‡] Department of Chemistry.

[§] Present address: SECOR International Incorporated, Springfield, IL 62702.

TABLE 1. Experiments Performed and Typical Concentrations in Drinking Water

exp. no.	added solutes	solute concn. (mg/L) ^a	initial [NO ₃ ⁻] (mg/L as N)	initial [NO ₂ ⁻] (mg/L as N)	typical solute concn. in drinking water ^c
1	none (DNW)		30	0	
2	carbonic acid	720	30	0	0–220 ^d
3	carbonic acid (pH=6.3)	720	30	0	0–220 ^d
4	bicarbonate	398	30	0	2–300 ^d
5	bicarbonate	835	30	0	2–300 ^d
6	carbonate	180	30	0	0–15 ^d
7	chloride, carbonic acid	50, 720	30	0	0–250 ^e
8	chloride, carbonic acid	1000, 720	30	0	0–250 ^e
9	sulfate, carbonic acid	680, 720	30	0	0–1000 ^f
10	sulfate, carbonic acid	1374, 720	30	0	0–1000 ^f
11	sulfite, carbonic acid	0.5, 720	30	0	NA
12	sulfite, carbonic acid	5, 720	30	0	NA
13	sulfide, bicarbonate	0.2, 398	30	0	0–1 ^g
14	sulfide, bicarbonate	0.4, 398	30	0	0–1 ^g
15	humic acid, carbonic acid	3.3 ^c , 720	30	0	0.1–10 ^h
16	groundwater, carbonic acid (unfiltered)	(Table 2), 720	30	0	
17	groundwater, carbonic acid (filtered)	(Table 2), 720	30	0	
18	groundwater (unbuffered)	(Table 2)	30	0	
19	groundwater, carbonic acid (PAC)	(Table 2)	30	0	
20	carbonic acid (regenerated-low)	720	30	0	0–220 ^d
21	carbonic acid (regenerated-high)	720	30	0	0–220 ^d
22	carbonic acid	720	0	30	0–220 ^d
23	chloride, carbonic acid	1000, 720	0	30	0–250 ^e
24	sulfite, carbonic acid	5, 720	0	30	NA
25	carbonic acid (regenerated-low)	720	0	30	0–220 ^d
26	carbonic acid (regenerated-high)	720	0	30	0–220 ^d

^a Solute concentrations are written in order as listed in adjacent column. All concentrations (unless otherwise noted) are in mg/L as solute.

^b Phosphate reported in mg/L as P. ^c Represents range for first solute listed. ^d Stumm and Morgan (34) assuming a pH range of 6.0–9.0. ^e 250 mg/L Cl⁻ represents secondary MCL set by U.S. EPA. ^f Trembaczowski (35). ^g Minnesota Department of Health (36). ^h Thurman (37) reported as DOC in mg/L as C. NA = values were not available in the literature.

2. Experimental Section

2.1 Catalyst Preparation and Characterization. Pd–Cu/γ-Al₂O₃ (5 wt % Pd, 1.5 wt % Cu) catalysts were prepared following conventional methods (32). Details of the catalyst preparation method are provided in the Supporting Information. Pd–Sn and Pd–In catalysts were prepared in a way similar to that of Pd–Cu catalysts, but initial tests determined that Pd–Cu catalysts exhibited a higher NO₃⁻ reduction rate and less NH₃ production. Therefore, only Pd–Cu catalysts were used in this study.

The prepared catalyst was analyzed for surface area, pore volume, and pore size distribution using N₂ gas adsorption at 77 K (Micromeritics, ASAP 2010). Surface area was determined by the BET method, and pore volume and pore size distribution were determined by the Horvath–Kawazoe model (33). Powder X-ray diffraction (XRD) measurements were performed to characterize the metallic phases present on the catalyst.

2.2 Reagents. Tanks of H₂ (99.999%) and CO₂ (99.9%) were purchased from Matheson Tri-Gas (Joliet, IL). Carbonic acid in solution was provided by the CO₂ and concentrations were determined based on the partial pressure of CO₂ and the solution pH. All chemicals were reagent-grade sodium salts (Fisher or Sigma-Aldrich). Humic acid was used as a surrogate for dissolved organic matter (DOM) in natural waters (Alfa Aesar). The deionized, Nanopure water (DNW) was tap water purified by ion exchange (resistivity 16 megohm cm at 25° C) and then filtered through a Nanopure water system (Barnstead) to achieve a product water with resistivity of 18 megohm cm (25 °C).

2.3 Reactor System. The reactor used to test the reaction kinetics of the catalysts was a 0.6 L clear glass (Pyrex) bottle maintained at atmospheric pressure and at a temperature of 21±0.1 °C by submerging the reactor in a constant temperature water bath. The reactor was equipped with a

pH probe and datalogger that recorded pH and temperature (WTW, Weilheim, Germany). For each experiment, approximately 0.5 L of water was added to the reactor, followed by catalyst addition. Hydrogen (135 mL/min), and in most cases, CO₂ (70 mL/min) were bubbled into the system via 1/16 in. Teflon tubing. A detailed description of the experimental setup and control experiments is provided in the Supporting Information.

2.4 Analytical Methods. Nitrate and nitrite were analyzed using ion chromatography (Dionex ICS-2000; Dionex IonPac AS18 column; 36 mM KOH eluent; 1 mL/min eluent flow rate). Ammonia was measured using a gas sensitive probe (Orion 9512), after raising the pH of the sample to 13 by NaOH addition (detection limit of 0.03 mg/L as N). Analyses of natural water samples and elemental analyses of catalysts were performed using ICP-MS by the Department of Chemistry Microanalysis Laboratory (University of Illinois at Urbana-Champaign). Dissolved organic carbon (DOC) concentrations were measured using a total organic carbon (Dohrmann, Phoenix 8000) analyzer. Sulfide (HS⁻) was tested using a Chemets colorimetric test kit (Cole-Parmer) with an accuracy of ±0.1 mg/L HS⁻. The pH was measured using a pH electrode (SenTix 41, WTW). Nitrous oxide was analyzed on an HP-6890a GC equipped with a Carboxen 1004 stainless steel micropacked column (Supelco) and a TCD detector.

2.5 Nitrate and Nitrite Reduction Experiments. A complete list of the experiments performed is given in Table 1. Concentrations of carbonate species were calculated by the total carbonate added and the final solution pH. Concentrations used in the experiments were close to the upper limit of values found in drinking water sources. In the case of Cl⁻, much higher values were chosen to mimic engineered treatment systems (e.g., effluent from ion exchange system).

Experiments were also performed with a natural groundwater sample amended with NO₃⁻; the solution composition

TABLE 2. Solute Concentrations in Groundwater Sample

solute	raw groundwater (mg/L)	PAC treated groundwater (mg/L)
carbonate	5.21	13.39
bicarbonate	206	202
carbonic acid	0.85	0.30
chloride	1.0	1.9
sulfate	1.1	0.3
sulfite	<0.5	<0.5
sulfide ^a	<0.1	<0.1
phosphate ^b	0.062	<0.02
DOC ^c	2.88	0.64
NO ₃ ⁻	0.14	0.02
pH	8.21	9.16
ammonia (as N)	2.00	1.85
calcium	38.56	30.60
magnesium	27.39	26.50
sodium	35.00	35.00
silica	15.08	10.10
potassium	1.59	2.96
total dissolved iron	0.20	0.03

^a Accuracy of sulfide concentrations is ± 0.1 mg/L. ^b Phosphate reported in mg/L as P. ^c DOC reported in mg/L as C.

before and after pretreatment with PAC is listed in Table 2. The groundwater sample was taken from a well adjacent to the Newmark Civil Engineering Laboratory (University of Illinois at Urbana-Champaign), and was tested under the following scenarios: unfiltered, filtered (0.45 μ m), buffered with CO₂, unbuffered, and after pretreatment with PAC (WPH Pulv, Calgon). A control experiment (exp 3) was also performed at a pH similar to that of the buffered groundwater by sparging with CO₂ and adding NaOH. All NO₃⁻ and NO₂⁻ reduction experiments were performed in duplicate.

2.6 Kinetic Modeling. A single site Langmuir–Hinshelwood–Hougen–Watson (LHHW) model was used to account for NO₃⁻ and NO₂⁻ reduction including competition for reactive sites (eq 4).

$$\frac{dC_{\text{NO}_3^-}}{dtC_{\text{cat}}} = - \frac{k_{\text{NO}_3^-} K_{\text{NO}_3^-} K_{\text{H}_2}^{0.5} C_{\text{NO}_3^-} C_{\text{H}_2}^{0.5}}{1 + K_{\text{NO}_3^-} C_{\text{NO}_3^-} + \sum K_i C_i} \quad (4)$$

where C represents aqueous concentration (mg/L), $k_{\text{NO}_3^-}$ is the zero order rate constant for NO₃⁻ reduction (mg N/g cat min), $K_{\text{NO}_3^-}$ is the adsorption constant for NO₃⁻ (L/mg N), K_{H_2} is the adsorption constant for H₂ (L/mg), and $\sum K_i C_i$ accounts for all nonreactive adsorbed species. Kinetic formulations similar to eq 4 have been used to model nitrate reduction using Pd bimetallic catalysts (8, 10, 20). Since variation in the hydrogen partial pressure and purge rate did not affect NO₃⁻ reduction rates (Supporting Information), the H₂ terms in eq 4 can be absorbed into the rate constant and eq 4 becomes

$$\frac{dC_{\text{NO}_3^-}}{dtC_{\text{cat}}} = - \frac{k_{\text{NO}_3^-} K_{\text{NO}_3^-} C_{\text{NO}_3^-}}{1 + K_{\text{NO}_3^-} C_{\text{NO}_3^-} + \sum K_i C_i} \quad (5)$$

where $k_{\text{NO}_3^-}$ is the apparent zero order rate constant for NO₃⁻ reduction (mg N/g cat min). Equation 5 can also be used when NO₂⁻ is the starting reactant instead of NO₃⁻; the subscript NO₃⁻ is replaced with NO₂⁻.

Scientist for Windows (v. 2.01, Micromath Research, St. Louis, MO) was used for kinetic modeling. Values for $k_{\text{NO}_3^-}$ and $K_{\text{NO}_3^-}$ were obtained by fitting eq 5 to the experimental data for experiments 1 and 2 while holding $\sum K_i C_i$ fixed at zero. When competitive ions were present, values obtained for $k_{\text{NO}_3^-}$ and $K_{\text{NO}_3^-}$ from experiment 1 were held fixed and

fits were obtained by varying the value for $\sum K_i C_i$. To facilitate comparison among data, observed first-order rate constants normalized by the catalyst concentration (k_{obs} (L/min g catalyst)) were determined by linear regression of plots of $\ln(\text{concentration})$ vs time for NO₃⁻ conversion of up to 50%. In all cases, duplicate data sets were combined and simultaneously fit. The same approach was used for fitting NO₂⁻ concentration profiles.

3. Results and Discussion

3.1 Catalyst Characterization. Gas adsorption for the prepared catalyst gave a surface area of 122 m²/g (BET method). The pore volume and average pore diameter were 0.25 cm³/g and 10.7 nm, respectively. Elemental analysis revealed that the freshly prepared catalyst contained amounts of Pd and Cu very close to the theoretical values (Table 3). Only trace amounts of other elements were detected, with the exception of Cl. The elevated Cl concentration was likely the result of the preparation method by the manufacturer, as lower levels were observed for catalysts rinsed with DNW. The catalysts were chemically stable over a pH range of 5.0–11.5, since changes in Pd and Cu content were not observed during experiments 1–6. Results from XRD measurements showed peaks consistent with fcc Pd–Cu alloy particles, however no peaks for separate Pd or Cu phases were observed, as previously reported using this preparation method (32).

3.2 Carbonate Species and pH. Observed first-order rate constants and final NO₂⁻ and NH₃ concentrations for NO₃⁻ and NO₂⁻ reduction experiments are listed in Table 4. Typical concentration profiles for a NO₃⁻ reduction experiment are shown in the Supporting Information (Figure S-4). Based on prior work (18), the balance of NO₃⁻ is assumed to be reduced to N₂ and small amounts of N₂O (Supporting Information). Nitrate reduction profiles for the carbonate species (H₂CO₃, HCO₃⁻, and CO₃²⁻) and unbuffered experiments are shown in the Supporting Information (Figures S-5 and S-6). Corresponding observed first-order rate constants are documented in Table 4. Nitrate reduction rates decrease corresponding to increases in HCO₃⁻ concentrations, and the final NO₂⁻ concentration increased from carbonic acid to bicarbonate to carbonate, in order of increasing pH (Supporting Information, Figure S-6). These results are consistent with previous reports that HCO₃⁻ adsorbs to NO₃⁻ active sites on the catalyst and decreases the reduction rate (10, 12, 14, 16). An increase in NO₂⁻ concentrations corresponding to pH has also been observed in other studies (7, 10, 13, 14, 16, 18, 19, 21, 24), and has been attributed to adsorption of OH⁻ ions to NO₂⁻ reduction sites and deprotonation of the catalyst surface resulting in a negative surface charge that repels NO₂⁻ ions (24).

Since the NO₃⁻ reduction rate was not significantly different for the unbuffered and CO₂ buffered experiments, it can be concluded that the pH change and the low HCO₃⁻ concentration present in experiment 2 had no significant effect on NO₃⁻ reduction kinetics. Also, no NO₂⁻ was present at the end of experiment 2. For these reasons, experiment 2 will be used as the base case for which all other experiments will be compared.

The final NO₂⁻ and NH₃ concentrations increased in the unbuffered experiment. A mass balance of nitrogen containing compounds from the unbuffered DNW experiment indicates that all NO₃⁻ was reduced to either NO₂⁻ or NH₃ (102% recovery). This result indicates that losses of NH₃ were likely small even at elevated pH. Contrary to previous reports (7, 10, 12–14, 16, 18, 19, 21), our results indicate that higher pH does not shift the reaction pathway from eq 2 to eq 3. The production of NH₃ seems to be more dependent on the presence or absence of a pH buffer, as was previously suggested (38). When a pH buffer is present (experiments 2–6), NH₃ production is between 17 and 36% of NO₃⁻

TABLE 3. Results of Elemental Analyses of Catalysts^a

exp. no.	sample	Pd wt %	Cu wt %	C wt %	H wt %	N wt %	Cl wt %	S wt %	Ca wt %	Fe wt %
NA	fresh PdCu catalyst	5.02	1.48	0.10	0.13	0.01	0.75	0.03	0.07	ND
8	chloride 1000 mg/L	5.20	1.25	0.13	0.14	0.02	0.23	ND	ND	ND
NA	humic acid (Alpha Aesar)			29.40	2.76	0.65			1.07	1.09
15	humic acid 3.3 mg/L as C	4.77	1.50	1.43	0.15	0.14	0.41	0.09	0.68	0.09
17	GW (filtered)	4.62	2.07	1.09	0.15	0.10	0.06	0.04	0.25	0.03
16	GW (unfiltered)	4.57	2.48	1.10	0.20	0.11	0.05	0.26	0.36	1.30
19	GW PAC	4.88	1.56	0.33	0.09	0.07	0.46	0.06	0.12	0.04
10	sulfate 1374 mg/L	5.01	1.23				0.13	0.16		
12	sulfite 5 mg/L	4.69	1.36	0.26	0.12	0.10	0.20	0.67	0.08	0.02
14	sulfide 0.4 mg/L	5.00	1.50				0.053	0.53		
20	low regeneration	5.11	1.00	0.13	0.09	0.03	0.11	0.17	ND	ND
21	high regeneration	4.87	0.55	0.50	0.16	0.10	0.30	0.08	0.14	0.01

^a ND = not detected, NA = not applicable since no catalyst present.TABLE 4. NO₃⁻ Activity for Solute Experiments and Final NO₂⁻ and NH₃ Concentrations

exp. no.	added solutes	<i>k</i> _{obs} ^a (L/min g cat)	final ^b NO ₂ ⁻ (mg/L)	avg. % ^c NO ₂ ⁻	final ^b NH ₃ (mg/L)	avg. % ^c NH ₃	pH ^e
1	none (DNW) ^d	2.52 × 10 ⁻⁰¹ (1.33 × 10 ⁻⁰²)	14.8, 14.7	48.9	15.3, 17.1	53.0	7.4–11.5
2	carbonic acid	2.36 × 10 ⁻⁰¹ (2.38 × 10 ⁻⁰²)	0, 0	0	8.8, 8.5	29.0	5.1–6.1
3	carbonic acid	1.37 × 10 ⁻⁰¹ (5.92 × 10 ⁻⁰³)	0, 0	0	10.6, 10.6	35.2	6.3–6.5
4	bicarbonate	1.20 × 10 ⁻⁰¹ (1.34 × 10 ⁻⁰²)	14.3, 14.6	60.6	8.6, 9.5	35.9	9.1–10.1
5	bicarbonate	8.73 × 10 ⁻⁰² (4.68 × 10 ⁻⁰³)	11.8, 13.5	52.4	8.0, 7.8	29.4	9.2–9.9
6	carbonate	1.47 × 10 ⁻⁰¹ (1.15 × 10 ⁻⁰²)	22.2, 22.2	75.7	4.5, 5.4	16.5	11.2–11.4
7	chloride, carbonic acid	8.35 × 10 ⁻⁰² (3.36 × 10 ⁻⁰²)	0, 0	0	6.8, 6.2	23.9	5.1–6.1
8	chloride, carbonic acid	2.25 × 10 ⁻⁰³ (1.28 × 10 ⁻⁰³)	0, 0	0	0.8, 1.0	40.9	5.1–5.3
9	sulfate, carbonic acid	1.81 × 10 ⁻⁰¹ (8.89 × 10 ⁻⁰³)	0, 0	0	11.3, 10.8	33.0	5.1–6.1
10	sulfate, carbonic acid	1.36 × 10 ⁻⁰¹ (5.45 × 10 ⁻⁰³)	0, 0	0	8.8, 10.3	32.6	5.1–6.1
11	sulfite, carbonic acid	8.99 × 10 ⁻⁰² (1.13 × 10 ⁻⁰²)	0.1, 0.2	0.6	5.7, 6.0	22.2	5.1–6.0
12	sulfite, carbonic acid	no reduction	0, 0	0	0, 0	0	5.0–5.1
13	sulfide, bicarbonate	2.36 × 10 ⁻⁰² (2.29 × 10 ⁻⁰³)	9.9, 10.3	80.3	0.4, 1.5	12.5	9.3–9.6
14	sulfide, bicarbonate	7.96 × 10 ⁻⁰³ (9.33 × 10 ⁻⁰⁴)	2.8, 3.9	63.7	0.3, 0.5	7.9	9.1–9.5
15	humic acid, carbonic acid	4.07 × 10 ⁻⁰² (7.41 × 10 ⁻⁰³)	0.09, 0.08	0.5	5.8, 7.2	42.0	5.3–5.9
16	groundwater, carbonic acid (unfiltered)	4.10 × 10 ⁻⁰³ (4.75 × 10 ⁻⁰⁴)	0, 0	0	1.7, 1.6	71.1	6.5–6.5
17	groundwater, carbonic acid (filtered)	3.67 × 10 ⁻⁰³ (6.05 × 10 ⁻⁰⁴)	0, 0	0	1.5, 1.6	73.0	6.5–6.5
18	groundwater (unbuffered)	4.81 × 10 ⁻⁰³ (3.91 × 10 ⁻⁰⁴)	1.6, 1.5	58.9	0.8, 1.0	28.6	8.9–9.3
19	groundwater, carbonic acid (PAC)	5.06 × 10 ⁻⁰² (3.76 × 10 ⁻⁰⁴)	0.05, 0.04	0.2	11.6, 11.3	57.7	6.3–6.4
20	carbonic acid (regenerated-low)	1.95 × 10 ⁻⁰³ (2.67 × 10 ⁻⁰⁴)	0, 0	0	0.5, 0.4	33.7	5.1–5.3
21	carbonic acid (regenerated-high)	2.04 × 10 ⁻⁰² (9.49 × 10 ⁻⁰⁴)	0, 0	0	1.1, 1.2	11.0	5.1–5.7
22	carbonic acid (NO ₂ ⁻)	5.07 × 10 ⁻⁰¹ (3.88 × 10 ⁻⁰²)	0, 0		5.5, 4.6	19.5	5.0–6.0
23	chloride, carbonic acid (NO ₂ ⁻)	2.00 × 10 ⁻⁰¹ (8.69 × 10 ⁻⁰³)	0, 0		3.2, 2.5	13.1	5.1–6.0
24	sulfite, carbonic acid (NO ₂ ⁻)	9.35 × 10 ⁻⁰³ (6.74 × 10 ⁻⁰³)	23.7, 23.2		0.3, 0.2	19.0	6.0–6.3
25	carbonic acid (NO ₂ ⁻) (regenerated-low)	9.98 × 10 ⁻⁰² (4.14 × 10 ⁻⁰³)	14.8, 15.1		1.8, 1.7	13.3	5.0–5.8
26	carbonic acid (NO ₂ ⁻) (regenerated-high)	3.22 × 10 ⁻⁰¹ (3.04 × 10 ⁻⁰²)	0, 0		1.4, 1.5	5.6	5.1–6.0

^a Values in parentheses represent ±95% confidence intervals for *k*_{obs}. ^b Represent values from duplicate experiments. Concentrations represent mg/L as N. ^c Normalized to amount of NO₃⁻ reduced in NO₃⁻ reduction experiments and normalized to amount of NO₂⁻ reduced in NO₂⁻ reduction experiments. ^d No buffer is added in experiment 1. ^e pH values represents initial and final.

reduced. However, when no buffer is used (experiment 1) NH₃ production is 53%. These results suggest that a pH buffer can prevent the accumulation of OH⁻ ions on the catalyst surface and thus decrease NH₃ production (38).

3.3 Humic Acid. Nitrate reduction profiles for the humic acid experiments are shown in the Supporting Information (Figure S-7), and observed first-order rate constants are documented in Table 4. Humic acid at a concentration of 3.3 mg/L as C resulted in a decrease in the NO₃⁻ reduction rate and small amounts of NO₂⁻. Nitrate was reduced 29% and 42% to NH₃, in the absence and presence of humic acid, respectively. Elemental analyses of the catalyst exposed to the humic acid solution are shown in Table 3. The results indicate that the catalyst has an elevated C and Ca content relative to the fresh catalyst. Elemental analyses showed that the humic acid powder contained significant quantities of C, Ca, and Fe (Table 4), indicating that humic acid adsorbed to the catalyst. Results for humic acid are the first experiments reported for this solute on Pd–Cu catalysts. We recognize

that the effects of humic acid on nitrate reduction may not adequately represent those of DOM; further tests with more complex DOM constituents are necessary.

3.4 Chloride. Nitrate and nitrite reduction profiles for chloride experiments are shown in the Supporting Information (Figures S-8 and S-9), and corresponding observed first-order rate constants are documented in Table 4. At a Cl⁻ concentration typical of drinking waters (50 mg/L), the NO₃⁻ reduction rate decreased by approximately 35%, NO₃⁻ was reduced 24% to NH₃, and no NO₂⁻ was detected. In the presence of high Cl⁻ concentrations (1000 mg/L, experiment 8), NO₃⁻ reduction was almost completely inhibited, NO₃⁻ was reduced 41% to NH₃, and no NO₂⁻ was detected.

Nitrite reduction experiments (i.e., nitrite is the starting reactant) conducted with Pd–Cu catalysts showed a decrease of over half in the NO₂⁻ reduction rate in the presence of 1000 mg/L Cl⁻, and NH₃ production was at 13% compared to 19% for the control case (experiment 22). The catalyst loading for NO₂⁻ reduction experiments was half that of NO₃⁻

reduction experiments, so the ratio of Cl^- to catalyst concentration was twice as high for NO_2^- reduction experiments compared to NO_3^- reduction experiments. Based on these results, it is evident that Cl^- inhibits NO_3^- reduction much more than NO_2^- reduction. This observation could be due to either preferential sorption of Cl^- to NO_3^- active sites (versus NO_2^- active sites), or accumulation of Cl^- over NO_3^- (but to a lesser extent over NO_2^-) in the Helmholtz layer. Pintar et al. (23) concluded that accumulation of Cl^- ions in the Helmholtz layer leads to the deprotonation of the catalyst surface and enhanced repulsion of NO_3^- ions resulting in reduced activity, but the authors did not look at NO_2^- reduction. Results from elemental analysis indicate that the catalyst–Cl interaction is likely weak since only low amounts of Cl atoms remained on the Pd–Cu catalyst after rinsing with DNW (Table 3). The Cu content of catalysts exposed to 1000 mg/L Cl^- were below the theoretical value of 1.5 wt % suggesting that some Cu dissolution occurred. The dissolution of Cu was previously observed in acidic H_2SO_4 and HCl solutions and was attributed to anion sorption to the Cu surface followed by dissolution (39).

3.5 Sulfur Species. The effect of sulfur species (HS^- , SO_3^{2-} , and SO_4^{2-}) on NO_3^- reduction is shown in the Supporting Information (Figures S-10 and S-11), and corresponding observed first-order rate constants are shown in Table 4. Carbon dioxide was used to control pH during SO_4^{2-} and SO_3^{2-} experiments. During HS^- experiments, NaHCO_3 was used to maintain the solution pH above the pK_a of $\text{H}_2\text{S}/\text{HS}^-$ (6.99), thereby avoiding the volatilization of HS^- as H_2S .

The NO_3^- reduction rates were less in the presence of SO_4^{2-} , SO_3^{2-} and HS^- , with HS^- and SO_3^{2-} having the greatest effect. Nitrate reduction rates further decreased with increasing SO_4^{2-} , SO_3^{2-} , and HS^- concentrations. The effect of SO_3^{2-} on NO_2^- reduction was also tested (experiment 24) and was found to be inhibitory. Sulfur compounds were added before NO_3^- or NO_2^- addition and after the pH had equilibrated. Upon addition of sulfur compounds an increase in pH was observed, suggesting a reaction with the catalyst surface occurred.

The reaction pathway was altered by the presence of different sulfur species. The presence of HS^- , but not SO_3^{2-} , caused the fraction of NO_3^- reduced to NO_2^- to increase, but not in proportion to HS^- concentrations. Both HS^- and SO_3^{2-} caused the fraction of NO_3^- reduced to NH_3 to decrease. Sulfite at 5 mg/L was also shown to inhibit NO_2^- reduction, but surprisingly did not affect NH_3 production (experiment 24).

Elemental analyses of sulfur fouled catalysts are shown in Table 3. Results show that catalysts exposed to SO_4^{2-} , SO_3^{2-} , and HS^- contained sulfur on the catalyst surface. The nitrate reduction rates for the three experiments decrease with increasing sulfur found on the catalyst surface. The catalyst exposed to 1374 mg/L SO_4^{2-} showed a lower content of Cu than the theoretical value, indicating Cu dissolution may have occurred.

All sulfur species tested in this study had an effect on NO_3^- reduction rates. The more reduced sulfur compounds showed an effect at the lowest concentrations. Both SO_3^{2-} and HS^- are known poisons of Pd catalysts (26, 28, 29), but our study is the first report of these ions fouling Pd–Cu bimetallic catalysts in the liquid phase. Since these ions are often present in natural waters, further research is necessary in catalyst or process design to minimize their negative effects.

3.6 Regeneration of Catalysts. Regeneration of Pd–Cu catalysts used during the SO_3^{2-} fouling experiments was attempted using two separate regeneration conditions. The catalyst was exposed to a hypochlorite solution of 750 mg/L for 2 h and 1500 mg/L for 22 h, both in batch mode. The catalysts were rinsed with DNW for 15 min and then tested for both NO_3^- and NO_2^- reduction in a solution buffered

with CO_2 . Hypochlorite was used because prior research has shown that it regenerated sulfur fouled Pd catalysts (28). Hypochlorite is thought to oxidize the bound sulfur into sulfate, which can then be rinsed off the catalyst surface. Results from the Pd–Cu catalyst regenerated under the low hypochlorite solution showed only a slight increase in the NO_3^- reduction rate. However, at the higher regenerant concentration a further increase in the NO_3^- reduction rate was observed, but the rate was only 10% of that observed in experiment 2. The regenerated Pd–Cu catalysts were also applied to NO_2^- reduction (experiments 25 and 26). Results from these experiments showed a significant increase in the NO_2^- reduction rate compared to the SO_3^{2-} fouled catalyst (experiment 24), and an increase in NH_3 . Nitrate and nitrite reduction profiles for these experiments are shown in the Supporting Information (Figures S-12 and S-13).

Results from elemental analysis of sulfite-fouled catalysts are shown in Table 3. The catalyst fouled by 5 mg/L SO_3^{2-} contained 0.67 wt % S. After regeneration the catalyst contained only 0.17 and 0.08 wt % S for the low and high regeneration conditions, respectively. The regenerated catalyst showed a significant decrease in Cu content, indicating that dissolution of Cu by the hypochlorite solution occurred. Further research is therefore needed to identify better regeneration conditions for Pd–Cu catalysts.

3.7 Natural Waters. Levels of dissolved constituents in the groundwater sample are shown in Table 2. An experiment (experiment 3) was also performed with DNW at a pH similar to that of the natural groundwater (pH = 6.3) to obtain a base case to compare the natural groundwater experimental results. Nitrate reduction profiles for the natural groundwater experiments and the base case are shown in the Supporting Information (Figure S-14), and corresponding first order rate constants are documented in Table 4. The nitrate reduction rates for filtered and unfiltered and buffered and unbuffered groundwater samples were not significantly different, but the rates were much lower than those of experiment 3. When the groundwater sample was buffered with CO_2 , NO_3^- was reduced 0% to NO_2^- and 71% to NH_3 . When no pH buffer was used, NO_3^- was reduced 59% to NO_2^- and 29% to NH_3 . The base case experiment showed that NO_3^- was reduced 0% to NO_2^- and 35% to NH_3 . These results show the necessity of using a pH buffer when treating natural waters in order to minimize NO_2^- concentrations.

Elemental analysis results of catalysts exposed to the groundwater sample are shown in Table 3. The catalyst used for the unfiltered groundwater sample (experiment 16) contained elevated levels of Cu, Ca, Fe, S, and C. Upon filtering the groundwater the catalyst still contained elevated levels of Cu, Ca, and C, but levels of Fe and S were present at only trace amounts. These results indicate that the Fe and S were present as solid mineral particulates. Since the NO_3^- reduction rate was not different for the filtered and unfiltered groundwater experiments, it is likely that Fe and S minerals did not adsorb directly to the catalyst. The high levels of C are attributed to natural organic matter (NOM) fouling of the catalyst, and the Ca and Cu are attributed to either mineral precipitation or are a result that these elements were coordinated to DOM. The precipitation of $\text{CaCO}_3(\text{s})$ onto the catalyst is a possible source of fouling because the concentrations of these ions in solution (Table 2) were on the same order of magnitude as the solubility limit.

The groundwater sample was also treated with a PAC loading of 500 mg/L for a period of 6 days in batch mode and was filtered through a 0.45 μm membrane to remove PAC particles. Total dissolved organic carbon (DOC) was reduced from 2.88 to 0.64 mg/L as C by PAC treatment. Nitrate reduction rates increased by a factor of approximately 6.2 after PAC treatment. Only small amounts of NO_2^- were detected in solution and NH_3 production decreased slightly.

TABLE 5. Modeling Constants from Fits of LHHW Model to Experimental Data^a

exp. no.	$k_{\text{NO}_3^-}$ (mg-N/g cat min)	$k_{\text{NO}_2^-}$ (mg-N/g cat min)	$K_{\text{NO}_3^-}$ (L/mg N)	$K_{\text{NO}_2^-}$ (L/mg N)	$\Sigma K_i C_i$ (dimensionless)	K_i (L/mg)	RSS
1	10.19 (2.75)		0.039 (0.017)		0 ^b		9.2
2	8.37 (1.07)		0.052 (0.012)		0 ^b		1.5
3	8.37 ^b		0.052 ^b		0.93 (0.07)	1.26×10^{-03c}	6.5
4	8.37 ^b		0.052 ^b		2.02 (0.13)	5.08×10^{-03c}	17.9
5	8.37 ^b		0.052 ^b		3.38 (0.20)	4.05×10^{-03c}	32.7
6	8.37 ^b		0.052 ^b		1.15 (0.11)	5.75×10^{-02c}	10.2
7	8.37 ^b		0.052 ^b		2.62 (0.27)	5.24×10^{-02}	28.7
8	8.37 ^b		0.052 ^b		147 (24)	1.47×10^{-01}	24.4
9	8.37 ^b		0.052 ^b		0.24 (0.03)	3.52×10^{-04}	1.9
10	8.37 ^b		0.052 ^b		1.06 (0.05)	7.71×10^{-04}	3.9
11	8.37 ^b		0.052 ^b		2.65 (0.26)	$5.30 \times 10^{+00}$	30.7
12	not modeled						
13	8.37 ^b		0.052 ^b		15.6 (1.2)	$6.79 \times 10^{+01}$	2.6
14	8.37 ^b		0.052 ^b		44.8 (3.0)	$1.07 \times 10^{+02}$	3.4
15	8.37 ^b		0.052 ^b		11.2 (1.1)	$3.39 \times 10^{+00}$	53.5
16	8.37 ^b		0.052 ^b		103 (7)		1.6
17	8.37 ^b		0.052 ^b		115 (11)		1.1
18	8.37 ^b		0.052 ^b		87.7 (3.7)		0.6
19	8.37 ^b		0.052 ^b		13.7 (0.5)		2.8
20	8.37 ^b		0.052 ^b		207 (34)		0.8
21	8.37 ^b		0.052 ^b		18.9 (0.6)		0.3
22		14.12 (2.97)		0.099 (0.051)	0 ^b		7.6
23		14.12 ^b		0.099 ^b	3.96 (0.15)	3.96×10^{-03}	7.8
24		14.12 ^b		0.099 ^b	147 (55)	$2.94 \times 10^{+01}$	2.2
25		14.12 ^b		0.099 ^b	10.5 (0.7)		3.9
26		14.12 ^b		0.099 ^b	0.52 (0.15)		12.2

^a Values in parentheses represent $\pm 95\%$ confidence intervals. ^b Held constant during modeling. ^c Adsorption constant calculated for bicarbonate.

Since only small amounts of S were detected on the catalyst surface it was assumed that sulfur species had little effect on NO_3^- reduction. The results of elemental analysis before and after PAC treatment indicate that the levels of C, Ca, and Cu decreased significantly due to PAC treatment. The removal of these elements corresponded to an increase in NO_3^- reduction rate indicating that they were responsible for catalyst fouling.

3.8 Kinetic Modeling. Based on eq 5, results from kinetic modeling provided values for $k_{\text{NO}_3^-}$, $K_{\text{NO}_3^-}$, and $\Sigma K_i C_i$ for NO_3^- reduction experiments, and values for $k_{\text{NO}_2^-}$, $K_{\text{NO}_2^-}$, and $\Sigma K_i C_i$ for NO_2^- reduction experiments (Table 5). The LHHW model presented in eq 5 was able to fit the experimental data with excellent accuracy throughout the entire time course of the experiments (Supporting Information), indicating that the use of the LHHW model incorporating competitive sorption was appropriate for representing the experimental data.

Adsorption constants (Table 5) were calculated for HCO_3^- , Cl^- , SO_4^{2-} , SO_3^{2-} , HS^- , and humic acid (Supporting Information). The calculated K_i values indicate that the adsorption of solutes to the Pd–Cu catalyst surface increase in approximately the following order: $\text{SO}_4^{2-} < \text{HCO}_3^- < \text{Cl}^- < \text{humic acid} < \text{SO}_3^{2-} < \text{HS}^-$. This ordering corresponds to the ability of these solutes to foul NO_3^- reduction as observed in this work. Adsorption constants (K_i) for individual solutes were comparable between experiments, except for HCO_3^- which varied by as much as an order of magnitude. This result indicates that other mechanisms not considered by the model may also be affecting adsorption of this solute.

3.9 Environmental Relevance. Results from our study show that NO_3^- was reduced below the regulatory MCL while producing NH_3 and small amounts of NO_2^- and N_2O (Supporting Information). Nitrite concentrations were maintained below the regulatory MCL when the solution pH was buffered by carbonic acid. However, NH_3 concentrations are still higher than the maximum permitted level for the European Community (0.5 mg/L as NH_4^+). Further research

is needed to identify more selective catalysts, and to develop engineered processes that address elevated NH_3 levels. In addition, alternant electron donors to H_2 should be explored to optimize the cost of this technology. Natural groundwater samples were shown to inhibit the catalytic NO_3^- reduction reaction. Catalytic NO_3^- reduction can be improved in natural waters by lowering the solution pH and placing the system after normal drinking water treatment processes (e.g., PAC treatment).

Acknowledgments

This work is supported in part by the Science and Technology Center program of the National Science Foundation under agreement number CTS-0120978. Acknowledgment also is made to the donors of the Petroleum Research Fund, administered by the American Chemical Society, for partial support of this research, and to Keith Hurley for his work on the XRD catalyst characterization.

Supporting Information Available

A description of the catalyst preparation method, control experiments conducted, reactor setup, discussion of N_2O measurements, discussion of kinetic modeling, figures of model fits, and figures of experimental data are available in the supporting information. This material is available free of charge via the Internet at <http://pubs.acs.org>.

Literature Cited

- United States Environmental Protection Agency. *National Water Quality Inventory*; EPA 816-R-00-013; USEPA Office of Water: Washington, DC, August 2000.
- Comly, H. H. Cyanosis in infants caused by nitrate in well water. *J. Am. Med. Assoc.* **1945**, *129* (2), 112–116.
- Weyer, P. J.; Cerhan, J. R.; Kross, B. C.; Hallberg, G. R.; Kantamneni, J.; Breuer, G.; Jones, M. P.; Zheng, W.; Lynch, C. F. Municipal drinking water nitrate level and cancer risk in older women: The Iowa women's health study. *Epidemiology* **2001**, *12* (3), 327–338.

- (4) United States Environmental Protection Agency. *National Primary Drinking Water Regulations: Contaminant Specific Fact Sheets, Inorganic Chemicals, Technical Version*; 811-F-95-002a-T; USEPA Office of Water, Washington, DC, October 1995.
- (5) Urbain, V.; Benoit, R.; Manem, J. Membrane bioreactor: A new treatment tool. *J. Am. Water Works Assoc.* **1996**, *5*, 75–85.
- (6) Kapoor, A.; Viraraghavan, T. Nitrate removal from drinking water-review. *J. Environ. Eng.-ASCE* **1997**, *123* (4), 371–380.
- (7) Hördel, S.; Vorlop, K.-D.; Tacke, T.; Sell, M. Development of catalysts for a selective nitrate and nitrite removal from drinking water. *Catal. Today* **1993**, *17* (1–2), 21–30.
- (8) Pintar, A.; Batista, J.; Levec, J.; Kajiuchi, T. Kinetics of the catalytic liquid-phase hydrogenation of aqueous nitrate solutions. *Appl. Catal. B: Environ.* **1996**, *11* (1), 81–98.
- (9) Strukul, G.; Pinna, F.; Marella, M.; Meregalli, L.; Tomaselli, M. Sol–gel palladium catalysts for nitrate and nitrite removal from drinking water. *Catal. Today* **1996**, *27* (1–2), 209–214.
- (10) Pintar, A.; Šetinc, M.; Levec, J. Hardness and salt effects on catalytic hydrogenation of aqueous nitrate solutions. *J. Catal.* **1998**, *174* (1), 72–87.
- (11) Daum, J.; Vorlop, K.-D. Kinetic investigation of the catalytic nitrate reduction: Construction of the test reactor system. *Chem. Eng. Technol.* **1999**, *22* (3), 199–202.
- (12) Pintar, A. and Batista, J. Catalytic hydrogenation of aqueous nitrate solutions in fixed-bed reactors. *Catal. Today* **1999**, *53* (1), 35–50.
- (13) Prüsse, U.; Hähnlein, M.; Daum, J.; Vorlop, K.-D. Improving the catalytic nitrate reduction. *Catal. Today* **2000**, *55* (1–2), 79–90.
- (14) Deganello, F.; Liotta, L. F.; Macaluso, A.; Venezia, A. M.; Deganello, G. Catalytic reduction of nitrates and nitrites in water solution on pumice-supported Pd–Cu catalysts. *Appl. Catal. B: Environ.* **2000**, *24* (3–4), 265–273.
- (15) Ilinitich, O. M.; Nosova, L. V.; Gorodetskii, V. V.; Ivanov, V. P.; Trukhan, S. N.; Gribov, E. N.; Bogdanov, S. V.; Cuperus, F. P. Catalytic reduction of nitrate and nitrite ions by hydrogen: investigation of the reaction mechanism over Pd and Pd–Cu catalysts. *J. Mol. Catal. A: Gen.* **2000**, *158* (1), 237–249.
- (16) Matatov-Meytal, Yu.; Barekko, V.; Yuranov, I.; Kiwi-Minsker, L.; Renken, A.; Sheintuch, M. Cloth catalysts for water denitrification: II. Removal of nitrates using Pd–Cu supported on glass fibers. *Appl. Catal. B: Environ.* **2001**, *31* (4), 233–240.
- (17) Pintar, A.; Batista, J.; Levec, J. Integrated ion exchange/catalytic process for efficient removal of nitrates from drinking water. *Chem. Eng. Sci.* **2001**, *56* (4), 1551–1559.
- (18) Yoshinaga, Y.; Akita, T.; Mikami, I.; Okuhara, T. Hydrogenation of nitrate in water to nitrogen over Pd–Cu supported on active carbon. *J. Catal.* **2002**, *207* (1), 37–45.
- (19) Gavagnin, R.; Biasetto, L.; Pinna, F.; Strukul, G. Nitrate removal in drinking waters: the effect of tin oxides in the catalytic hydrogenation of nitrate by Pd/SnO₂ catalysts. *Appl. Catal. B: Environ.* **2002**, *38* (2), 91–99.
- (20) Lemaigen, L.; Tong, C.; Begon, V.; Burch, R.; Chadwick, D. Catalytic denitrification of water with palladium-based catalysts supported on activated carbons. *Catal. Today* **2002**, *75* (1–4), 43–48.
- (21) Mikami, I.; Sakamoto, Y.; Yoshinaga, Y.; Okuhara, T. 2003 Kinetic and adsorption studies on the hydrogenation of nitrate and nitrite in water using Pd–Cu on active carbon support. *Appl. Catal. B: Environ.* **2003**, *44* (1), 79–86.
- (22) Palomares, A. E.; Prato, J. G.; Rey, F.; Corma, A. Using the “memory effect” of hydrotalcites for improving the catalytic reduction of nitrates in water. *J. Catal.* **2004**, *221* (1), 62–66.
- (23) Pintar, A.; Batista, J.; Mušević, I. Palladium–copper and palladium–tin catalysts in the liquid-phase nitrate hydrogenation in a batch-recycle reactor. *Appl. Catal. B: Environ.* **2004**, *52* (1), 49–60.
- (24) Prüsse, U.; Vorlop K.-D. Supported bimetallic palladium catalysts for water-phase nitrate reduction. *J. Mol. Catal. A: Chem.* **2001**, *173* (1–2), 313–328.
- (25) Oudar, J. Sulfur adsorption and poisoning of metallic catalysts. *Catal. Rev.-Sci. Eng.* **1980**, *22*, 171.
- (26) Schreier, C. G.; Reinhard, M. Catalytic hydrodehalogenation of chlorinated ethylenes using palladium and hydrogen for the treatment of contaminated water. *Chemosphere* **1995**, *31* (6), 3475–3487.
- (27) Gravil, P. A.; Toulhoat, H. Hydrogen, sulphur and chlorine coadsorption on Pd(111): a theoretical study of poisoning and promotion. *Surf. Sci.* **1999**, *430* (1–3), 176–191.
- (28) Lowry, G. V.; Reinhard, M. Pd-Catalyzed TCE dechlorination in Groundwater: Solute effects, biological control, and oxidative catalyst regeneration. *Environ. Sci. Technol.* **2000**, *34* (15), 3217–3223.
- (29) Schüth, C.; Disser, S.; Schüth, F.; Reinhard, M. Tailoring catalysts for hydrodechlorinating chlorinated hydrocarbon contaminants in groundwater. *Appl. Catal. B: Environ.* **2000**, *28* (3–4), 147–152.
- (30) Bartholomew, C. Mechanisms of catalyst deactivation. *Appl. Catal. A: Gen.* **2001**, *212* (1–2), 17–60.
- (31) Gu, B.; Schmitt, J.; Chen, Z.; Liang, L.; McCarthy, J. F. Adsorption and desorption of natural organic matter on iron oxide: mechanisms and models. *Environ. Sci. Technol.* **1994**, *28* (1), 38–46.
- (32) Pintar, A.; Batista, J.; Aréon, I.; Kodre, A. Characterization of γ -Al₂O₃ Pd–Cu bimetallic catalysts by EXAFS, AES, and kinetic measurements. In *Preparation of Catalysts*; B. Delmon, P. A. Jacobs, R. Maggi, J. A., Martens, P., Grange, G., Poncelet, Eds.; Elsevier Science, Amsterdam; 1998; vol. 7.
- (33) Horvath, G.; Kawazoe, K. Method for the calculation of effective pore size distribution in molecular sieve carbon. *J. Chem. Eng. Jpn.* **1983**, *16*, 470–475.
- (34) Stumm, W.; Morgan, J. J. *Aquatic Chemistry: An Introduction Emphasizing Chemical Equilibria in Natural Waters*, 2nd ed.; John Wiley and Sons: New York, 1981.
- (35) Trembaczowski, A. Sulphur and oxygen isotopes behavior in sulphates of atmospheric groundwater system observations and model. *Nordic Hydrol.* **1991**, *22*, 49–66.
- (36) Minnesota Department of Health. *Hydrogen Sulfide and Sulfur Bacteria in Well Water*. <http://www.health.state.mn.us/divs/eh/wells/hydrosulfide.html>.
- (37) Thurman, E. M. *Organic Geochemistry of Natural Waters*; Kluwer Academic: Dordrecht, Netherlands, 1985.
- (38) D'Arino, M.; Pinna, F.; Strukul, G. Nitrate and nitrite hydrogenation with Pd and Pt/SnO₂ catalysts: The effect of the support porosity and the role of carbon dioxide in the control of selectivity. *Appl. Catal. B: Environ.* **2004**, *53*, 161–168.
- (39) Vogt, M. R.; Lachenwitzer, A.; Magnussen, O. M.; Behm, R. J. In-situ STM study of the initial stages of corrosion of Cu(100) electrodes in sulfuric and hydrochloric acid solution. *Surf. Sci.* **1998**, *399*, 49–69.

Received for review December 18, 2005. Revised manuscript received February 27, 2006. Accepted February 28, 2006.

ES0525298